SEMARAK ILMU PUBLISHING

Semarak Journal of Thermal-Fluid Engineering

Journal homepage:
https://semarakilmu.my/index.php/sjotfe/index
ISSN: 3030-6639

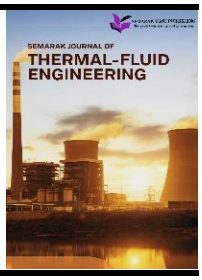

Analysis of Airflow Through a Porous Gas Mask Filter Cartridge

Muhammad Hamizan Azli[1], Ishkrizat Taib[2*], Muhammad Iqbal Zahin Arsam[1], Muhammad Iqram Hafiz Rusnizam[1], Muhammad Izzul Afif Mohd Nazaruddin[1], Nur Izzat Naqiuddin Nur Hisham[1], Muhammad Hazimuddin Halif[1]

[1] Fakulty of Mechanical and Manufacturing Engineering, Universiti Tun Hussein Onn Malaysia, 86400 Parit Raja, Johor, Malaysia
[2] UTHM-INTEKMA Advanced Industrial Modelling, Fakulty of Mechanical and Manufacturing Engineering, Universiti Tun Hussein Onn Malaysia, 86400 Parit Raja, Johor, Malaysia

ARTICLE INFO

Article history:
Received 16 January 2026
Received in revised form 6 February 2026
Accepted 6 March 2026
Available online 31 March 2026

Keywords:
Gas mask filter cartridge; porous media; airflow analysis; pressure drop; breathing resistance

ABSTRACT

Gas mask filter cartridges are essential protective devices that prevent the inhalation of hazardous gases and airborne contaminants while maintaining acceptable breathing comfort, where airflow behaviour through the porous filter material strongly influences pressure drop and breathing resistance. The aim of this study is to analyse airflow characteristics through a porous gas mask filter cartridge using Computational Fluid Dynamics (CFD) to evaluate the effects of inlet velocity and filter thickness on airflow performance. A three-dimensional model of the filter cartridge was developed and simulated using ANSYS Fluent under steady, incompressible, and isothermal conditions. The porous filter was modelled using a homogeneous porous media approach with a porosity of 0.8. Three inlet velocities of 1.0 m/s, 1.5 m/s, and 2.0 m/s were applied to represent different breathing intensities, while three filter thicknesses of 28 mm, 30 mm, and 32 mm were investigated. The results show that increasing filter thickness leads to higher flow resistance, causing greater pressure drops and reduced airflow velocity within the porous region. Quantitatively, a pressure drop of approximately 279 Pa was obtained at an inlet velocity of 1.0 m/s, with pressure losses increasing consistently as inlet velocity and filter thickness increased. The 32 mm filter produced the highest pressure drop and lowest airflow velocity, whereas the 28 mm filter showed the lowest resistance but may compromise filtration effectiveness. Overall, the 30 mm medium-thickness filter provided the most balanced performance by maintaining acceptable airflow while avoiding excessive pressure loss. These findings demonstrate that CFD is an effective tool for evaluating airflow behaviour and supporting the optimisation of gas mask filter cartridge design.

1. Introduction

Gas masks are widely used as personal protective equipment to protect users from inhaling harmful gases, vapours, aerosols, and fine particulate matter [1]. They are commonly applied in industrial workplaces, healthcare environments, emergency response operations, and military

* *Corresponding author.*
E-mail address: iszat@uthm.edu.my

https://doi.org/10.37934/sjotfe.8.1.1022a

applications. The main function of a gas mask is to ensure that the air inhaled by the user is safe for breathing [2]. This protection is mainly provided by the filter cartridge, which is an essential component of the gas mask system. The filter cartridge typically consists of porous materials such as fibrous filters and activated carbon, which allow air to flow through while removing hazardous contaminants from the air stream [3].

The performance of a gas mask filter cartridge is strongly influenced by airflow behaviour inside the porous filter material [4]. When air flows through the porous structure, resistance is generated due to friction and flow interaction within the pores. This resistance causes a pressure drop across the filter, which directly affects breathing comfort [5]. A high-pressure drop can make breathing difficult and lead to fatigue during prolonged use, while a low pressure drop improves comfort and usability. In addition, uniform airflow distribution across the filter is important to ensure that the entire filter area is effectively utilized. Non-uniform airflow may reduce filtration efficiency and cause uneven loading of the filter material, which can shorten the service life of the cartridge [6].

The problem addressed in this study is the difficulty in analysing airflow behaviour and pressure drop inside porous gas mask filter cartridges using experimental methods alone [7]. The complex internal structure of the porous filter makes direct measurement of velocity and pressure challenging, while experimental testing requires high cost and long development time. High airflow resistance can lead to breathing discomfort, and uneven airflow distribution may reduce filter effectiveness. As a result, a reliable and efficient numerical method is required to evaluate airflow characteristics inside gas mask filter cartridges and support performance assessment and design improvement.

Airflow through porous media is complex and depends on several factors, including porosity, permeability, filter thickness, and airflow rate [8]. As air passes through the interconnected pores of the filter material, energy losses occur, resulting in changes in velocity and pressure. Understanding these flow characteristics is essential for improving gas mask filter design and performance [9]. However, studying airflow inside porous filter cartridges using experimental methods is challenging. The internal structure of the filter is very fine and complex, making it difficult to directly measure velocity and pressure within the porous material. Experimental testing is often limited to measuring inlet and outlet pressure, while detailed internal flow information remains inaccessible [10]. Furthermore, experimental studies can be expensive and time-consuming, especially when multiple design variations need to be evaluated.

Due to these limitations, there is a need for an alternative approach that can effectively analyse airflow behaviour inside gas mask filter cartridges [11]. Computational Fluid Dynamics (CFD) has become a widely used numerical tool for analysing fluid flow in complex systems [12]. CFD solves the governing equations of fluid motion using numerical methods, allowing detailed prediction of velocity fields, pressure distribution, and flow resistance. Unlike experimental methods, CFD enables visualization of airflow inside porous filter materials, providing valuable insight into internal flow behaviour. As a result, CFD has been increasingly applied in the design and analysis of air filtration systems, including gas mask filter cartridges [13].

In CFD simulations, porous filter materials are commonly modelled using a porous media approach [14]. Instead of explicitly modelling the detailed microstructure of the filter fibres, the porous media model represents the resistance of the material using macroscopic properties such as permeability and inertial resistance coefficients [15]. This approach significantly reduces computational cost while still producing reliable predictions of pressure drop and airflow distribution [16]. Many previous studies have successfully applied porous media models to simulate airflow through gas mask canisters and respirator filters, demonstrating the effectiveness of CFD in predicting aerodynamic performance.

Although previous research has shown that CFD is a useful tool for analysing gas mask filters, many studies focus mainly on filtration efficiency and contaminant removal [17]. Fewer studies provide detailed discussion of airflow characteristics such as velocity distribution and pressure drop under simplified steady-state conditions. For educational and engineering design purposes, simplified CFD models are valuable because they allow fundamental airflow behaviour in porous filters to be clearly understood without excessive modelling complexity [18]. Therefore, further numerical studies focusing on airflow resistance and internal flow distribution in porous gas mask filter cartridges are still needed.

The objective of this study is to analyse airflow through a porous gas mask filter cartridge using Computational Fluid Dynamics. This study aims to simulate steady-state airflow inside a three-dimensional filter cartridge model using ANSYS Fluent, evaluate the airflow velocity distribution within the porous media, and determine the pressure drop across the filter under inhalation conditions. The porous filter material is modelled using a homogeneous and isotropic porous media approach to represent flow resistance without resolving the detailed microstructure. The analysis focuses on airflow behaviour only and does not consider chemical reactions or particle filtration mechanisms.

2. Methodology

2.1 Cartridge Geometry and Material Characterization

Rather than replicating the filter's physical shape, we use actual geometric information for the gas mask filter cartridge, including its inlet, outlet and porous filler region. The porous medium, which stands for the filter filler material, for these key material properties like porosity, permeability, and thickness, we depend on manufacturer data or literature. These properties are especially important when representing airflow resistance within the cartridge. Figure 1 show the gas mask filter cartridge.

Fig. 1. Gas mask filter cartridge [19]

For this study, three different substrate thicknesses were selected for the gas mask filter cartridge: 32 mm, 30 mm, and 28 mm. These thicknesses represent typical variations in filter design. The inlet body (C) and outlet body (A) dimensions were kept constant across all three cases to isolate the effect of the substrate thickness (B) as the sole variable. A three-dimensional, full-body model of the entire filter cartridge was created, including the inlet body (C), substrate (B), and outlet body (A). This approach, using a complete 3D model rather than exploiting symmetry, was adopted to capture any potential three-dimensional flow asymmetries in the turbulent flow field, ensuring a more thorough and physically representative simulation. As shown in Figure 2, this method provides a comprehensive representation of the geometry and flow domains within the filter cartridge system.

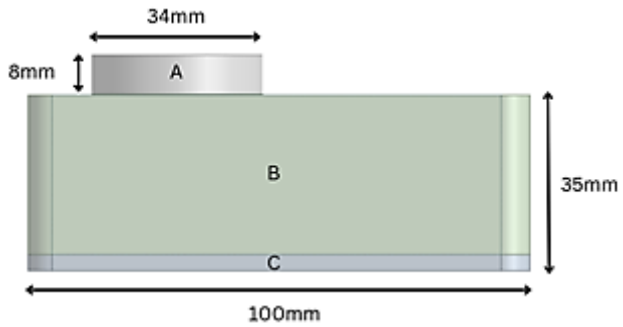

Fig. 2. gas mask filter cartridge geometry domain

2.2 Discretization

The computational domain for the gas mask filter cartridge is discretized into a finite number of small control volumes to allow the governing flow equations to be solved numerically. The discretization process converts the continuous form of the continuity and momentum equations into algebraic equations that can be handled by the CFD solver. A finer mesh is applied within and near the porous filter region to accurately capture steep velocity and pressure gradients caused by flow resistance inside the filter material. Regions close to the inlet and outlet of the cartridge also use refined elements to properly represent flow development and pressure changes. Coarser mesh elements are applied in regions where airflow is more uniform, such as open flow zones away from the porous media. This mesh strategy ensures accurate prediction of airflow distribution and pressure drop across the gas mask filter while keeping the computational cost at a reasonable level, as reported in [20].

2.2.1 Generate mesh

Mesh generation was carried out to discretize the computational domain into a finite number of control volumes for numerical analysis. An automated meshing method was applied to ensure consistent element distribution throughout the model. A uniform mesh size was used across most regions, while relatively finer elements were applied near the inlet, outlet, and porous filter region where higher velocity and pressure gradients were expected. This meshing strategy allows accurate prediction of airflow behaviour and pressure drop within the gas mask filter cartridge while maintaining reasonable computational efficiency. The generated mesh was checked to ensure acceptable quality in terms of element size and distribution before proceeding with the CFD simulations.

Mesh generation was performed using an automated meshing process. Body sizing controls were applied to specify the base element size in the converging section, with finer elements applied around the throat and exit, where high velocity gradients and strong shear were expected. Figure 3 shows the meshing of the gas mask filter cartridge. The mesh generation for the model was conducted using an automated process, with a mesh size of 1.2 mm applied across the entire domain. The model's dimensions, as shown, include sections labelled A, B, and C. No converging section or throat was used in this model. The finer mesh elements were applied near the exit region, where high velocity gradients and strong shear are expected. Figure 3 illustrates the mesh distribution of the model with consistent element size throughout.

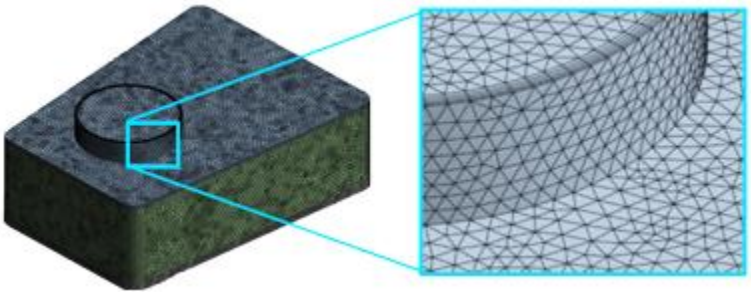

Fig. 3. Meshing of the gas mask filter cartridge

2.3 Governing Equation

Computational Fluid Dynamics (CFD) describes fluid flow behaviour using governing equations derived from fundamental conservation laws. For the analysis of airflow through a porous gas mask filter cartridge, these equations are essential for predicting air movement, pressure drop, and flow resistance inside the filter material. The three main governing equations are the continuity equation (mass conservation), the momentum equation (Navier–Stokes), and the energy equation (energy conservation). This study mainly focuses on mass and momentum conservation because airflow is assumed to be incompressible and occurs at constant temperature.

2.3.1 Continuity equation (mass conservation)

The conservation of mass for airflow through the porous filter cartridge is expressed by the continuity equation shown in Eq. (1). This equation states that the rate of change of air density within a control volume, combined with the net mass flux leaving the volume, must be zero. For a gas mask filter, Eq. (1) ensures that air entering the cartridge either flows through the porous media or accumulates within it, without any artificial creation or loss of mass in the numerical model. CFD simulations apply the equation to maintain physically realistic airflow distribution inside the porous filter structure, which is essential for accurate prediction of velocity fields and pressure drop, as reported in [21].

$$\frac{\partial \rho}{\partial t} + \nabla \cdot (\rho u) \tag{1}$$

where ρ= fluid density, u= velocity vector t= time

2.3.2 Momentum equation (Navier–Stokes)

The conservation of momentum for airflow through the gas mask filter cartridge is described by the Navier–Stokes equation given in Eq. (2). This equation represents the balance between the rate of change of momentum and the forces acting on the air, including pressure forces, viscous resistance within the porous material, and body forces such as gravity. For porous filter analysis, Eq. (2) plays an important role in predicting airflow resistance and pressure loss across the cartridge. CFD calculations solve the equation to capture how pressure gradients drive airflow through the filter while viscous stresses oppose the motion due to the fine pore structure. Accurate solution of Eq. (2) allows assessment of breathing resistance and overall filter performance.

$$\rho\left(\frac{\partial \rho}{\partial t} + \nabla \cdot (\rho u)\right) = -\nabla p + \nabla \times \tau + \rho b \quad (2)$$

where p= pressure, τ= viscous stress tensor, b= body force per unit mass

2.4 Boundary Condition

The CFD simulations in this study were performed using air as the working fluid under steady-state and incompressible flow assumptions. These assumptions are widely adopted in respiratory flow and gas mask filtration analyses, where airflow velocities are relatively low and density variations are negligible [22],[23]. The primary boundary conditions employed in this work comprise a velocity inlet, a pressure outlet, a porous zone definition, and no-slip wall conditions. Such boundary condition selections are commonly used in CFD investigations of gas mask filters and protective cartridge systems to represent inhalation flow behaviour realistically [24],[25].

The gas mask filter region was modelled as a porous medium with a porosity value of 0.8. Modelling the filter as a porous zone enables the capture of pressure drop and flow resistance effects without explicitly resolving the complex micro-scale pore structure, which significantly reduces computational cost while maintaining accuracy [26]. At the inlet, a uniform velocity profile was imposed to represent different breathing intensities. Three inlet velocities were considered 1.0 m/s for parameter 1, 1.5 m/s for parameter 2, and 2.0 m/s for parameter 3 (Table 1). The use of velocity inlet conditions enables a consistent comparison of pressure loss and flow behaviour under varying airflow demands, as recommended in previous CFD studies on filter and porous media performance [14]. A turbulence intensity of 5% and a turbulent viscosity ratio of 10 were specified to represent moderate turbulence levels typically observed in inhalation flows [27].

The outlet, a pressure outlet boundary condition with a gauge pressure of 0 Pa was applied to provide a reference pressure condition, which is a standard approach in CFD analyses of internal flows and filtration systems [28]. All solid surfaces were modelled as stationary no-slip walls with a standard roughness model, which is essential for accurately predicting near-wall velocity gradients and pressure losses in porous filter applications.

Table 1
Boundary conditions for CFD simulation

Boundary	Type	Specification	Value
Inlet	Velocity inlet	Parameter 1	1.0 m/s
		Parameter 2	1.5 m/s
		Parameter 3	2.0 m/s
Porous zone	Fluid zone	Porosity	0.8
Outlet	Pressure outlet	Gauge pressure	0 Pa
Wall	Wall	No-slip condition	Stationary
		Roughness model	Standard

2.5 Parameter of Study

This study investigates the effect of airflow velocity and filter thickness on the airflow behaviour inside a porous gas mask filter cartridge. Two main parameters were selected to represent realistic breathing conditions and common filter design variations. The first parameter is inlet airflow velocity, which represents different breathing intensities during inhalation [29]. Three inlet velocities were applied at the velocity inlet boundary: 1.0 m/s, 1.5 m/s, and 2.0 m/s. These values were chosen to

simulate low, moderate, and high breathing rates. The inlet velocity directly influences the pressure drop across the filter and the airflow velocity distribution inside the porous media.

The second parameter is filter thickness, which affects the flow resistance within the porous region. Three different filter thicknesses were analysed which is 28 mm, 30 mm and 32 mm. All other geometric dimensions, material properties, and boundary conditions were kept constant to ensure that the effect of filter thickness could be evaluated independently [30]. By varying these two parameters, the study aims to identify how design and operating conditions influence airflow performance and breathing resistance.

2.6 Analysis of Study

The analysis of this study focuses on evaluating airflow characteristics inside the gas mask filter cartridge using CFD simulation results. The main flow variables analysed include pressure distribution, velocity distribution, and velocity streamlines within the computational domain [31]. Pressure analysis is performed to determine the pressure drop across the porous filter, which is an important indicator of breathing resistance. Higher pressure drop indicates greater resistance to airflow and reduced breathing comfort. Pressure contours are used to visualise how pressure changes from the inlet to the outlet for different filter thicknesses and inlet velocities.

Velocity analysis is conducted to examine the airflow velocity distribution inside and downstream of the porous filter. Velocity contours help identify regions of high and low airflow, as well as the influence of filter thickness on airflow reduction. In addition, velocity streamlines are analysed to observe airflow paths and flow uniformity through the filter cartridge. Streamline patterns provide qualitative insight into flow resistance, energy loss, and airflow disturbance caused by different filter designs. Comparison of results for all cases allows identification of the filter configuration that provides a balance between acceptable airflow and reasonable pressure drop. This analysis supports the selection of an optimal filter thickness that improves breathing comfort while maintaining effective airflow behaviour.

2.7 Grid Independence Test

A grid independence test was conducted to ensure that the CFD results were not influenced by mesh size. Several meshes with different element sizes were tested, and the pressure drop across the filter cartridge was used as the comparison parameter. Results showed only small differences between successive mesh refinements, indicating that the solution had reached grid independence. The selected mesh provides accurate results while maintaining reasonable computational efficiency.

2.8 Related Theory

Inlet velocity is defined as the speed of the air flowing toward the porous filter surface which is important in the assessment of breathing comfort and filtration efficiency. When air flows through porous media at low velocities and in a laminar manner, the relation between inlet velocity and pressure drop can be defined using Darcy's Law. For the airflow through fibrous filters like gas masks and respirator materials, Darcy's Law works as the flow is assumed to be incompressible, steady and dominated by viscous effects [32]. The inlet velocity is given by Eq. (3):

$$v = \frac{k}{\mu L} \Delta P \tag{3}$$

where ΔP(Pa) is the pressure drop across the porous filter, μ(Pa·s) is the dynamic viscosity of air, L(m) is the thickness of the porous medium, and k(m²) represents the permeability of the porous material.

The velocity defined in this equation is the superficial velocity which is computed from the total inlet section instead of the pore area. This is the standard approach in computational fluid dynamics (CFD) for the inlet boundary condition, as it streamlines the modelling process of flow in porous media. More significant inlet velocities will generate a higher pressure drop, which corresponds to greater breathing resistance [33]. Thus, it is necessary to control the inlet velocity in order to find an optimal point of trade-off between the filtration efficiency and the comfort of breathing.

3. Results

3.1 Grid Independence Test

A grid independence test (GIT) was executed using the velocity distribution to determine the optimal mesh size for the gas mask filter simulation. The relative error between two successive meshes was calculated using the Eq. (3), and the normalized relative error was found to be less than 5% for all samples. Grid-convergence was confirmed as the pressure difference and exit velocity profiles showed minimal changes when transitioning from medium to fine mesh. As shown in Table 2, the analysis of pressure differences supported this conclusion. The mesh size of 1.2 mm was identified as the best option since it exhibited the lowest error and the largest element size, ensuring a faster simulation run. Therefore, the 1.2 mm mesh size was selected for all subsequent runs, offering a good balance between accuracy and computational efficiency.

Table 2
Grid independence test based on pressure variation in the computational domain

Mesh size (mm)	Number of nodes	Pressure drops (pa)	Error (%)
1.2	164476	279.42453	-
1.1	197888	279.3534	0.03
1.0	242292	279.03108	0.12

The truncation error was calculated using Eq. (4) for each mesh configuration shown in Table 2, and the mesh that provided the lowest error while still maintaining reasonable computational efficiency was selected for the final simulations. This step ensures that the numerical results reflect the true physical behaviour of the flow, rather than artifacts introduced by the discretization process.

$$\text{Error}(\%) = \left|\frac{\text{A}-\text{B}}{\text{A}}\right| \times 100 \quad (4)$$

3.2 Pressure Distribution

Figure 4 shows the pressure contours for the three filter designs with different thicknesses which is thin, medium, and thick at inlet velocities of 1 m/s, 1.5 m/s, and 2 m/s. For all cases, a clear pressure gradient is observed from the inlet to the outlet, indicating pressure loss due to flow resistance within the porous filter. Higher pressure is consistently observed near the inlet region, followed by a gradual pressure decrease along the flow direction as air passes through the porous medium.

Relatively higher local pressure values are observed near the inlet region for the thin filter of Design 1, especially at higher inlet velocities. This behaviour is mainly caused by the thinner filter thickness, which leads to a more concentrated pressure build-up at the entrance of the porous zone. Despite this local pressure increase, Design 1 exhibits the lowest overall pressure drop across the porous region, indicating lower resistance to airflow.

A progressive increase in overall pressure drop is observed with increasing filter thickness in medium Design 2 and thick Design 3 at all inlet velocities. Design 3 experiences the highest-pressure accumulation near the inlet and the steepest pressure gradient across the porous filter. These results confirm that thicker filters impose greater resistance to airflow due to longer flow paths and increased viscous losses.

Higher inlet velocities from 1 m/s to 2 m/s result in increased pressure magnitudes for all filter thicknesses, reflecting greater flow momentum and resistance within the porous media. The general trend related to filter thickness remains consistent across all velocities. Agreement with porous flow theory is observed, where pressure drop is directly proportional to both flow velocity and porous medium thickness.

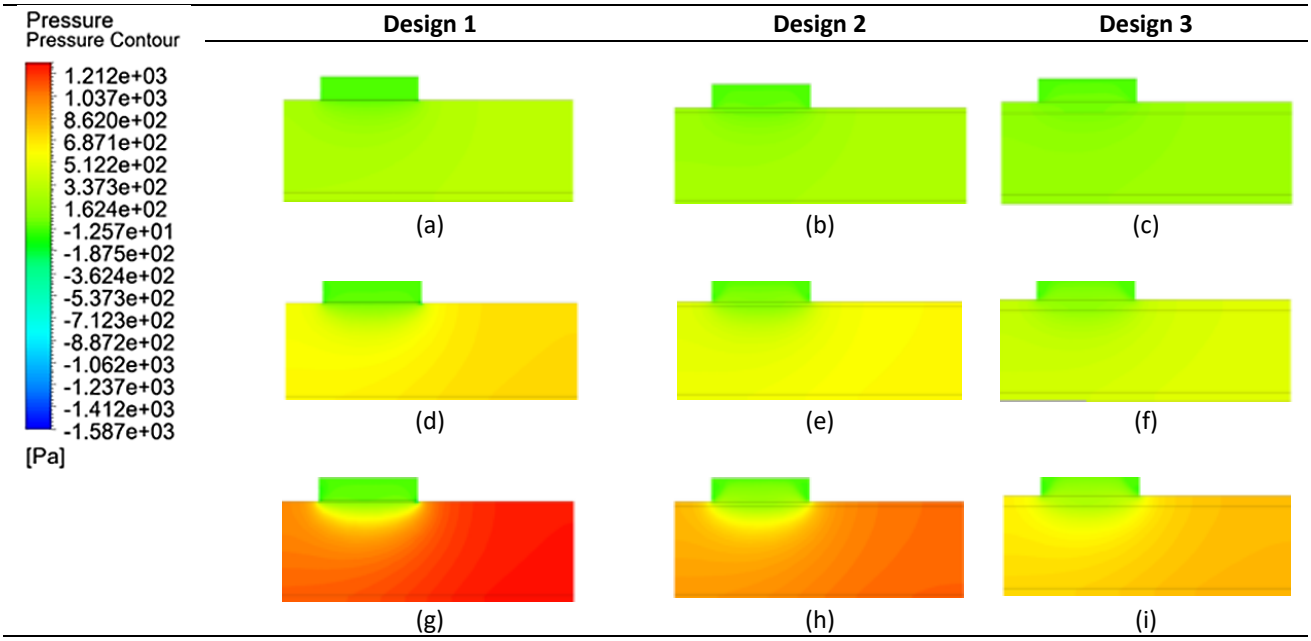

Fig. 4. Pressure contours of the gas mask filter cartridge for Design 1, Design 2, and Design 3 at inlet velocities (a)-(c) 1.0 m/s (d)-(f) 1.5 m/s (g)-(i) 2.0 m/s

3.3 Velocity Distribution

Figure 5 shows the velocity contours for all three filter designs with different thicknesses (thin, medium, and thick) at inlet velocities of 1 m/s, 1.5 m/s, and 2 m/s. In all cases, higher velocity regions are observed near the inlet and above the porous filter, followed by a reduction in velocity as the airflow passes through the porous medium. This velocity reduction indicates energy loss due to flow resistance within the filter.

Relatively higher velocity magnitudes are observed within and downstream of the porous region for the thin filter of Design 1 at all inlet velocities. This behaviour is attributed to the lower flow resistance associated with the thinner filter thickness, which allows air to pass through more easily. The velocity distribution in Design 1 also appears more uniform, indicating smoother airflow through the porous medium.

A noticeable reduction in airflow velocity occurs across the porous zone as the filter thickness increases in medium Design 2 and thick Design 3 configurations at all inlet velocities. Design 3 exhibits the lowest velocity magnitudes, confirming that thicker filters significantly restrict airflow. This reduction in velocity is consistent with the increased pressure drop observed in the pressure distribution results.

Higher inlet velocities from 1 m/s to 2 m/s produce increased velocity magnitudes near the inlet region for all designs, reflecting greater flow momentum. The overall trend remains consistent despite changes in inlet velocity, where increasing filter thickness leads to reduced airflow velocity. These findings indicate that filter thickness plays a dominant role in controlling airflow behaviour within the porous filter cartridge.

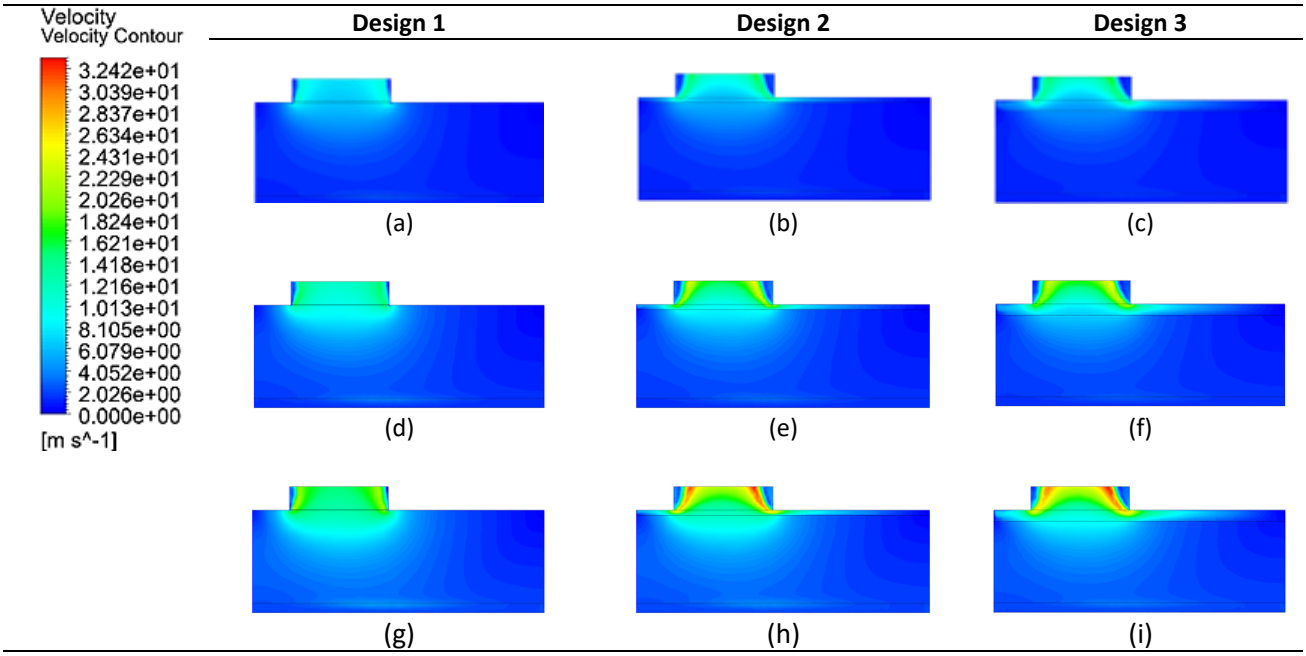

Fig. 5. Velocity contours of the gas mask filter cartridge for Design 1, Design 2, and Design 3 at inlet velocities (a)-(c) 1.0 m/s (d)-(f) 1.5 m/s (g)-(i) 2.0 m/s

3.4 Velocity Streamline Distribution

Figure 6 illustrates the velocity streamline patterns for all three filter designs with different thicknesses (thin, medium, and thick) at inlet velocities of 1 m/s, 1.5 m/s, and 2 m/s. The streamlines provide qualitative insight into airflow paths and flow uniformity as air passes through the porous filter cartridge. The streamlines for the thin filter of Design 1 are smoother and more evenly distributed as they enter and pass through the porous region at all inlet velocities. Minimal curvature and reduced streamline congestion are observed in the flow paths, indicating lower flow resistance and more stable airflow behaviour. This observation aligns with the higher velocity magnitudes and lower overall pressure drop reported in the previous sections.

Increasing the filter thickness causes the streamline patterns to become progressively denser near the inlet region, particularly above the porous filter. Greater streamline curvature and clustering appear, indicating higher flow resistance and greater energy loss as air moves through thicker, porous media. The most pronounced streamline distortion occurs in Design 3, confirming that it experiences the highest resistance to airflow.

Higher inlet velocities, from 1 m/s to 2 m/s, generate denser streamline patterns and stronger curvature near the inlet region for all filter thicknesses, reflecting increased flow momentum. Despite the effect of inlet velocity, the general trend regarding filter thickness remains consistent: thicker filters produce more restricted and disturbed airflow patterns. Overall, the streamline analysis supports the pressure and velocity distribution results, showing that increasing filter thickness leads to higher flow resistance and reduced airflow uniformity. These findings emphasise the importance

of selecting an optimal filter thickness to ensure acceptable airflow performance and breathing comfort.

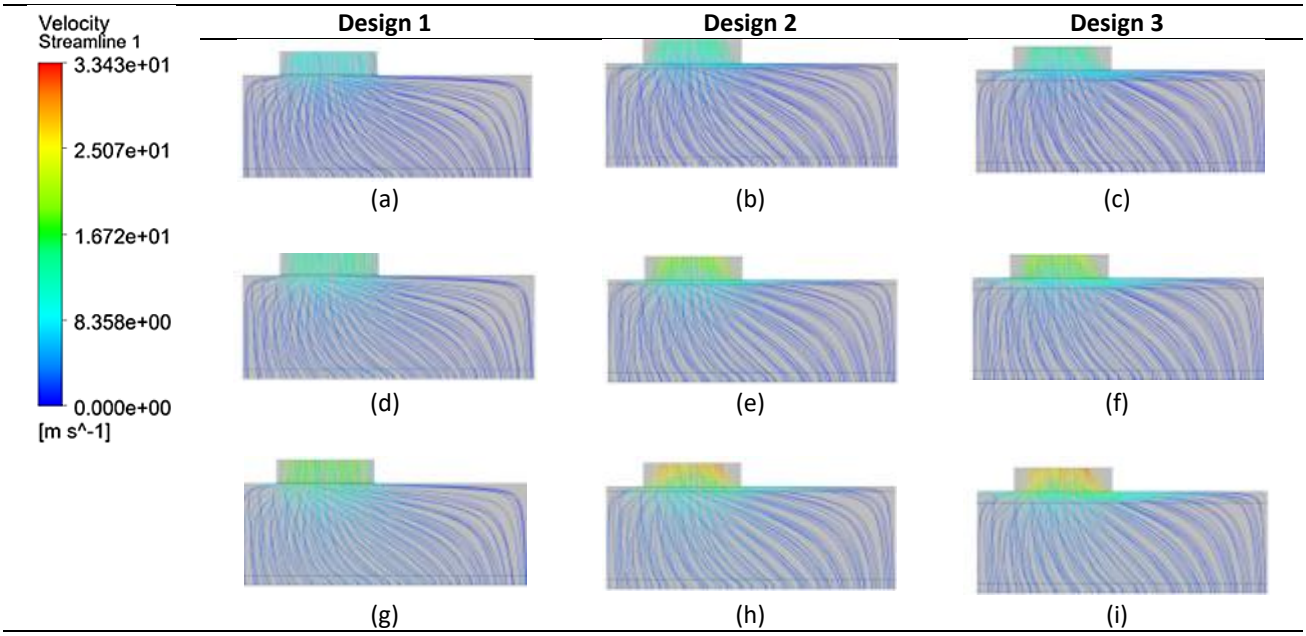

Fig. 6. Velocity streamline of the gas mask filter cartridge for Design 1, Design 2, and Design 3 at inlet velocities (a)-(c) 1.0 m/s (d)-(f) 1.5 m/s (g)-(i) 2.0 m/s

4. Conclusions

This study successfully achieved its objective of analysing airflow behaviour through a porous gas mask filter cartridge using Computational Fluid Dynamics. The CFD simulations effectively captured the pressure, velocity, and streamline characteristics of airflow through porous media at inlet velocities of 1 m/s, 1.5 m/s, and 2 m/s, demonstrating the suitability of CFD as a reliable tool for evaluating airflow performance in porous filter systems.

The results clearly indicate that filter thickness has a significant influence on airflow behaviour. Based on the combined pressure, velocity, and streamline analyses, thinner filters produce lower overall pressure drop, higher airflow velocity, and smoother streamline patterns, which contribute to improved breathing comfort. In contrast, thicker filters generate higher pressure loss, reduced airflow velocity, and more disturbed streamline behaviour due to increased flow resistance within the porous medium. Although increasing inlet velocity increases pressure and velocity magnitudes, the overall trend with respect to filter thickness remains consistent.

Among the three designs investigated, Design 1 (thin filter) exhibits the lowest pressure drop and highest airflow velocity, indicating superior breathing comfort, but its reduced thickness may limit filtration effectiveness. Design 3 (thick filter) shows the highest flow resistance and pressure loss, which may lead to breathing discomfort. Therefore, Design 2, with moderate filter thickness, provides the most balanced performance by maintaining acceptable airflow characteristics while avoiding excessive pressure loss, making it the most suitable design among the three for gas mask filter applications.

References

[1] Li, Chun-Chi. "Aerodynamic behavior of a gas mask canister containing two porous media." *Chemical Engineering Science* 64, no. 8 (2009): 1832-1843. https://doi.org/10.1016/j.ces.2009.01.009

[2] Su, Yin-Chia, and Chun-Chi Li. "Computational fluid dynamics simulations and tests for improving industrial-grade gas mask canisters." *Advances in Mechanical Engineering* 7, no. 8 (2015): 1687814015596297. https://doi.org/10.1177/1687814015596297
[3] Lawrence, Robert B., Matthew G. Duling, Catherine A. Calvert, and Christopher C. Coffey. "Comparison of performance of three different types of respiratory protection devices." *Journal of Occupational and Environmental Hygiene* 3, no. 9 (2006): 465-474. https://doi.org/10.1080/15459620600829211
[4] Jeon, Rakyoung, Shin Hyuk Kim, Kwangjun Ko, Kihyun Kwon, Myungkyu Park, Ireh Seo, Min Oh, and Chang-Ha Lee. "Advanced cartridge design for a gas respiratory protection system using experiments, CFD simulation and virtual reality." *Journal of Cleaner Production* 426 (2023): 139101. https://doi.org/10.1016/j.jclepro.2023.139101
[5] Zhang, Lydia, Mohamed K. Alshaikh, and Constantina Lekakou. "Assessment and design of filters and masks against COVID-19 via modeling and simulations." *Journal of Occupational and Environmental Hygiene* 21, no. 8 (2024): 576-590. https://doi.org/10.1080/15459624.2024.2357089
[6] Roberge, Raymond J., Emily Bayer, Jeffrey B. Powell, Aitor Coca, Marc R. Roberge, and Stacey M. Benson. "Effect of exhaled moisture on breathing resistance of N95 filtering facepiece respirators." *Annals of Occupational Hygiene* 54, no. 6 (2010): 671-677.
[7] Adli, Muhammad Aiman Rahimi. "Analysis of aircraft hydraulic filter flow: Computational fluid dynamics simulation using simflow 4.0." *Advanced and Sustainable Technologies (ASET)* 3, no. 2 (2024): 42-50. https://doi.org/10.58915/aset.v3i2.1432
[8] Oh, Geunwoo, Yesol Hyun, Jung-Il Choi, Jaeheon Lee, Min-Kun Kim, and Heesoo Jung. "Computational fluid dynamics modeling of contaminant transport with adsorption filtration inside planar-shaped air-purifying respirator canister." *Chemical Engineering Research and Design* 196 (2023): 171-183. https://doi.org/10.1016/j.cherd.2023.06.020
[9] Hinds, William C., and Yifang Zhu. *Aerosol technology: properties, behavior, and measurement of airborne particles*. John Wiley & Sons, 2022.
[10] Corbin, Joel C., Greg J. Smallwood, Ian D. Leroux, Jalal Norooz Oliaee, Fengshan Liu, Timothy A. Sipkens, Richard G. Green, Nathan F. Murnaghan, Triantafillos Koukoulas, and Prem Lobo. "Systematic experimental comparison of particle filtration efficiency test methods for commercial respirators and face masks." *Scientific Reports* 11, no. 1 (2021): 21979. https://doi.org/10.1038/s41598-021-01265-8
[11] Guo, Changzeng, Jian Kang, Desheng Wang, Yun Liang, Lingyun Wang, Guilong Xu, Hao Wang, and Min Tang. "Experimental and simulation study of particle deposition characteristics and pressure drop evolution in pleated filter media." *Processes* 13, no. 4 (2025): 975. https://doi.org/10.3390/pr13040975
[12] Versteeg, Henk Kaarle. *An introduction to computational fluid dynamics the finite volume method, 2/E*. Pearson Education India, 2007.
[13] Anderson, John D. *Computational fluid dynamics: the basics with applications*. New York: McGraw-Hill, 2015.
[14] ANSYS Inc. *ANSYS Fluent Theory Guide*. Canonsburg, PA: ANSYS Inc. 2023.
[15] Wang, Hongliang, and Pidong Shi. "Flow characteristic analysis of cfd-based air filter forward intake pipe." In *Journal of Physics: Conference Series*, vol. 1802, no. 2, p. 022015. IOP Publishing, 2021. https://doi.org/10.1088/1742-6596/1802/2/022015
[16] Korkmaz, Y. S., A. Kibar, and K. S. Yigit. "Experimental and numerical investigation of fluid flow in hydraulic filters." *Journal of Applied Fluid Mechanics* 15, no. 2 (2022): 363-371. https://doi.org/10.47176/jafm.15.02.32898
[17] Hou, Lei, Ayang Zhou, Xiao He, Wei Li, Yan Fu, and Jinli Zhang. "CFD simulation of the filtration performance of fibrous filter considering fiber electric potential field." *Transactions of Tianjin University* 25, no. 5 (2019): 437-450. https://doi.org/10.1007/s12209-019-00218-7
[18] Kummitha, Obula Reddy, R. Vijay Kumar, and V. Murali Krishna. "CFD analysis for airflow distribution of a conventional building plan for different wind directions." *Journal of Computational Design and Engineering* 8, no. 2 (2021): 559-569. https://doi.org/10.1093/jcde/qwaa095
[19] 3M 6006 Multi Gas Cartridge for 6000, 7000 (Pair). *Industrial Safety Products, accessed* January 31, 2026,
[20] Paris, Mathieu, Frédéric Dubois, Stéphane Bosc, and Philippe Devillers. "Integrating wind flow analysis in early urban design: Guidelines for practitioners." *Journal of Contemporary Urban Affairs* 7 (2023): 194-211. https://doi.org/10.25034/ijcua.2023.v7n2-12
[21] Blocken, Bert, and Ted Stathopoulos. "CFD simulation of pedestrian-level wind conditions around buildings: Past achievements and prospects." *Journal of Wind Engineering and Industrial Aerodynamics* 121 (2013): 138-145.
[22] Li, Chun-Chi. "Aerodynamic behavior of a gas mask canister containing two porous media." *Chemical Engineering Science* 64, no. 8 (2009): 1832-1843.. https://doi.org/10.1016/j.ces.2009.01.009
[23] Verma, Siddhartha, Manhar Dhanak, and John Frankenfield. "Visualizing the effectiveness of face masks in obstructing respiratory jets." *Physics of Fluids* 32, no. 6 (2020). https://doi.org/10.1063/5.0016018

[24] Sedlář, Milan, Tomáš Krátký, and Jiří Langer. "Numerical and experimental investigation of three-dimensional flow in combined protective canister filters." *Fluids* 7, no. 5 (2022): 171. https://doi.org/10.3390/fluids7050171
[25] Si, Fangfang, Pengfei Lian, Derui Yang, Guolin Han, Shaoyue Hao, and Pingwei Ye. "3D numerical simulation of aerodynamic characteristics of a gas filter." *Journal of Applied Mathematics and Physics* 7, no. 08 (2019): 1920. https://doi.org/10.4236/jamp.2019.78132
[26] Wojtasik-Malinowska, Justyna, Maciej Jaskulski, and Marcin Jaskulski. "CFD simulation of gas pressure drop in porous packing for rotating packed beds (RPB) CO." *Environmental Science and Pollution Research*, (2022). https://doi.org/10.1007/s11356-022-20859-x
[27] Durbin, P. "Turbulent Flows. By SB POPE. Cambridge University Press, 2000. 771 pp. ISBN 0 521 59886 9.£ 29.95 or 130.00 (hardback)." *Journal of Fluid Mechanics* 427 (2001): 410-411. https://doi.org/10.1017/S0022112000212913
[28] Anderson, John David, Gérard Degrez, Erik Dick, and Roger Grundmann. *Computational fluid dynamics: an introduction*. Springer Science & Business Media, 2013. https://doi.org/10.1007/978-3-662-11350-9
[29] Feng, Zhuangbo, Zhengwei Long, and Qingyan Chen. "Assessment of various CFD models for predicting airflow and pressure drop through pleated filter system." *Building and Environment* 75 (2014): 132-141. https://doi.org/10.1016/j.buildenv.2014.01.022
[30] Chen, Da-Ren, David YH Pui, and Benjamin YH Liu. "Optimization of pleated filter designs using a finite-element numerical model." *Aerosol Science and Technology* 23, no. 4 (1995): 579-590. https://doi.org/10.1080/02786829508965339
[31] Baléo, Jean-Noël, Albert Subrenat, and Pierre Le Cloirec. "Numerical simulation of flows in air treatment devices using activated carbon cloths filters." *Chemical Engineering Science* 55, no. 10 (2000): 1807-1816. https://doi.org/10.1016/S0009-2509(99)00441-8
[32] Darcy, Henry. "Les Fontaines Publiques de la Ville de Dijon." *Comptes Rendus de l'Académie des Sciences*, 1856.
[33] Nield, Donald A., and Adrian Bejan. *Convection in porous media*. New York, NY: Springer New York, 2006.